Supplementary Information

Transparent, Ultraflexible, and Superinsulating Nanofibrous Biocomposite Aerogels via Ambient Pressure Drying

*Guoqing Zu, * Sheng Zeng, Ben Yang, and Jia Huang*

Interdisciplinary Materials Research Center, Department of Polymeric Materials, School of Materials Science and Engineering, Tongji University, Shanghai 201804, P. R. China

*Email: guoqingzu@tongji.edu.cn

This PDF file includes:

Captions for Movies S1 to S4

Figures S1 to S14

Other Supplementary Materials for this manuscript includes the following:

Movies S1 to S4

Movie list:

Movie S1. High bending flexibility of TSP2 shown by hand bending.

Movie S2. Excellent machinability of TSP2 shown by cutting with a knife.

Movie S3. Real-time infrared thermal image of mineral wool (left), extruded polystyrene (middle), and TSP2 (right) on a hot plate from 15 s to 165 s.

Movie S4. Real-time infrared thermal image of mineral wool (left), extruded polystyrene (middle), and TSP2 (right) on ice from 0 s to 210 s.

Figures

Figure S1. Photograph of starch/polyorganosiloxane biocomposite aerogels obtained via APD. It is shown that the samples SP1 and SP2 are monolithic and optically opaque.

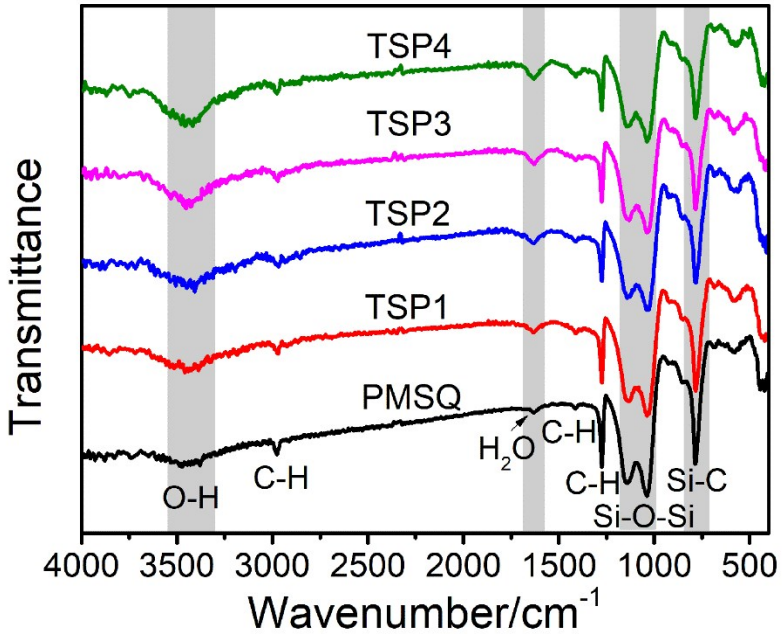

Figure S2. FTIR spectra of typical TOS/polyorganosiloxane biocomposite aerogels and PMSQ aerogels.

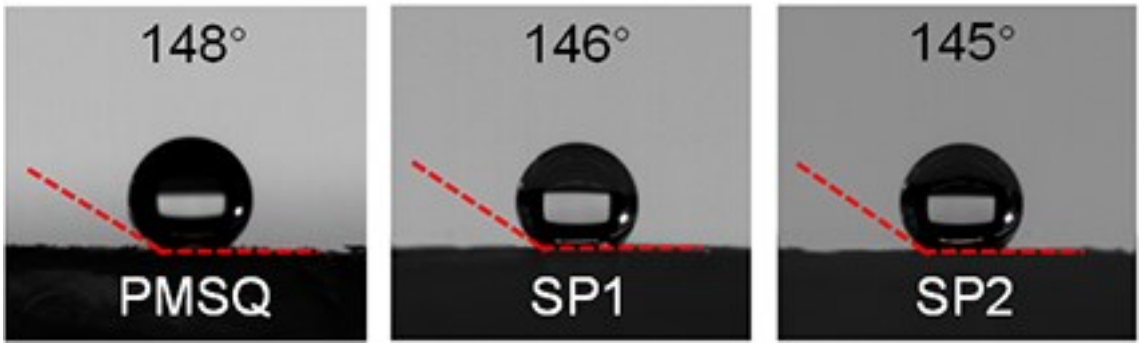

Figure S3. Water contact angles of the PMSQ aerogel and starch/polyorganosiloxane biocomposite aerogels (SP1 and SP2).

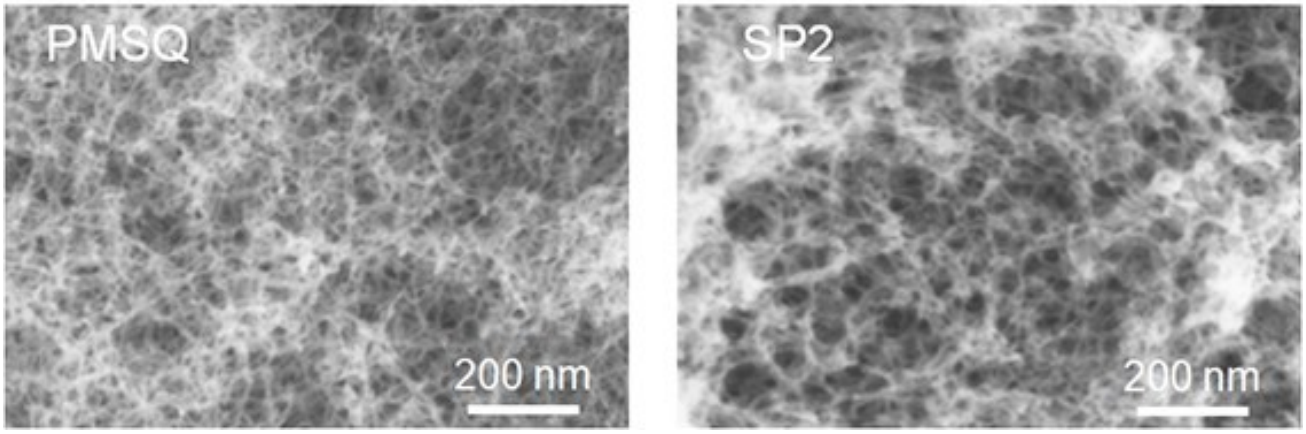

Figure S4. FESEM images of the PMSQ aerogel and starch/polyorganosiloxane biocomposite aerogel (SP2).

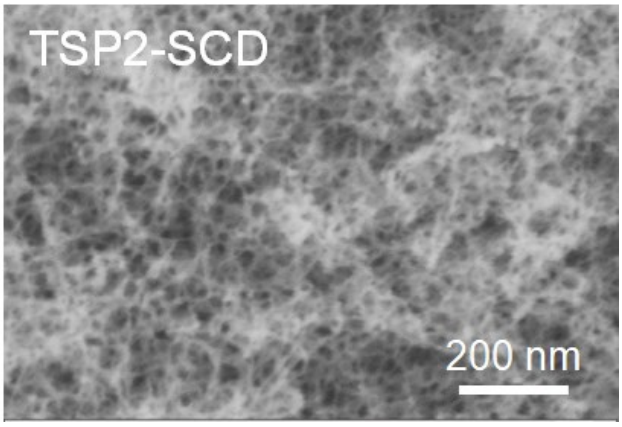

Figure S5. FESEM image of biocomposite aerogel TSP2-SCD obtained via SCD.

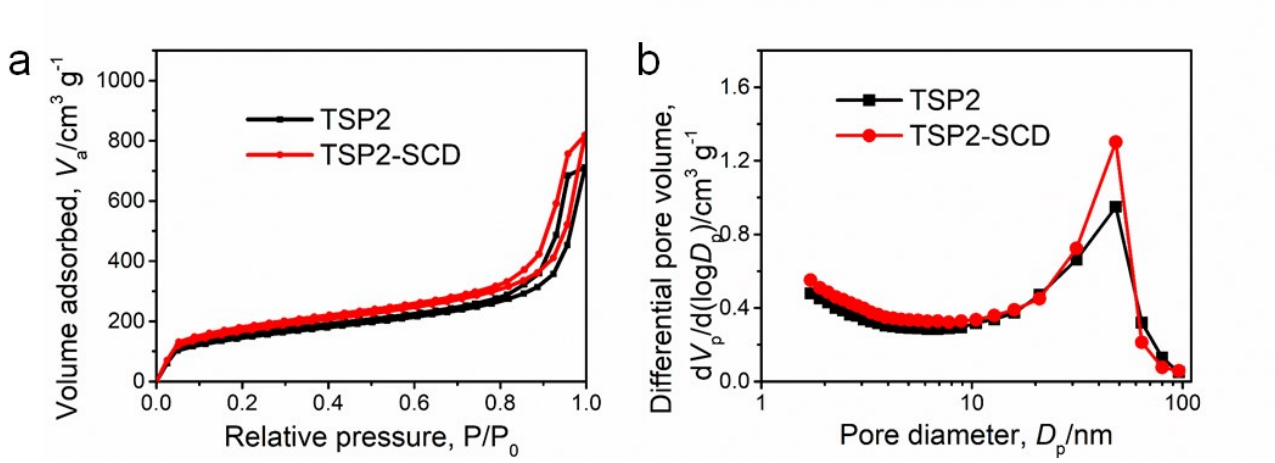

Figure S6. (a) Nitrogen adsorption/desorption isotherms and (b) pore size distributions of the biocomposite aerogels obtained via APD (TSP2) and SCD (TSP2-SCD).

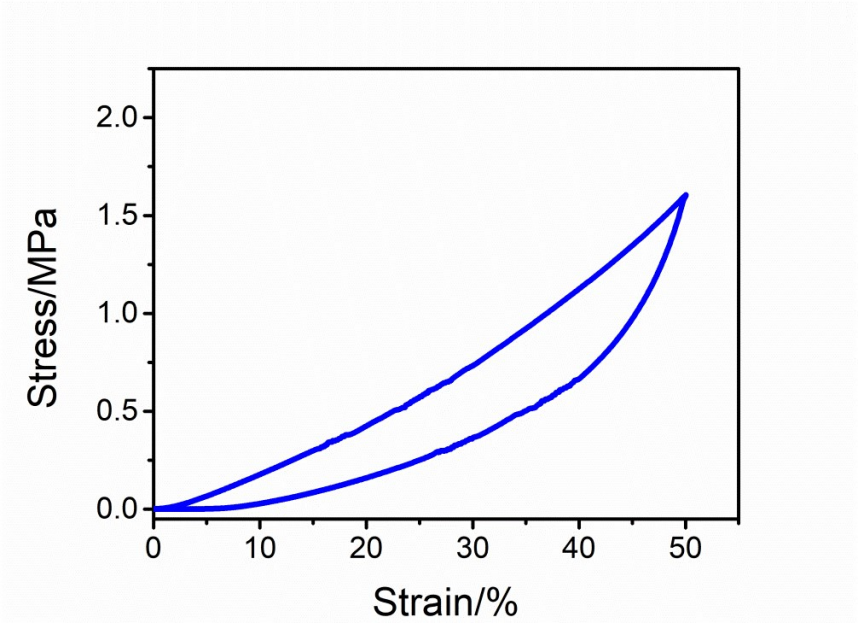

Figure S7. Stress-strain curve of a uniaxial compression-decompression test with 50% strain on SP2, showing high compressibility and elasticity.

Figure S8. Photographs of a hand bending test on SP2, which demonstrate that SP2 shows high bending flexibility.

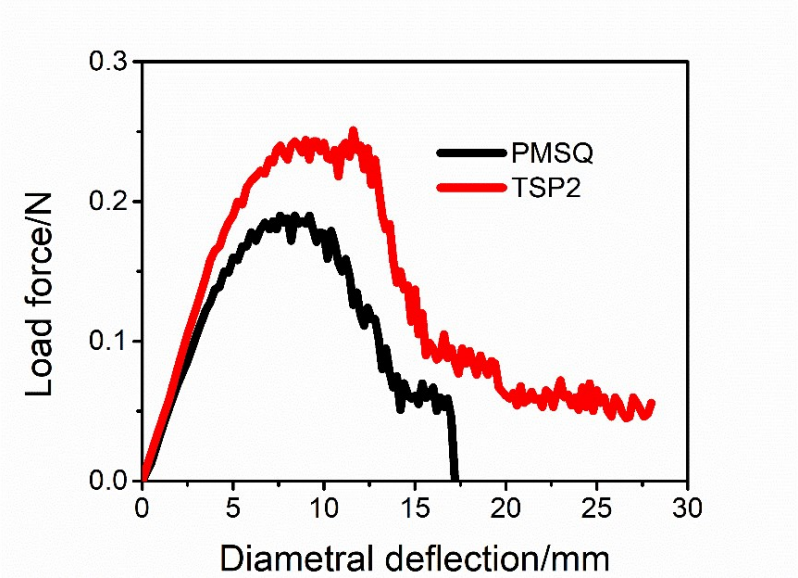

Figure S9. Stress-strain curves of three-point bending tests on TSP2 and the pristine PMSQ aerogel. The fixture span is 25 mm and a cuboid aerogel with typical width × length × height of 10 × 60 × 1 mm is used for the bending tests. TSP2 undergoes a large diametric deflection of 28 mm without fracture, whereas the pristine PMSQ aerogel is cracked under the diametric deflection of around 17 mm.

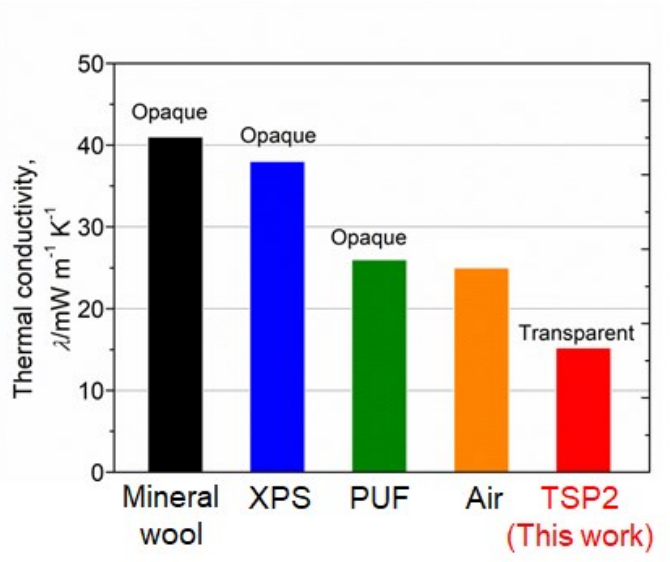

Figure S10. Comparison of thermal insulation performances of commercial thermally insulating materials[1] and the biocomposite aerogel TSP2 in this work.

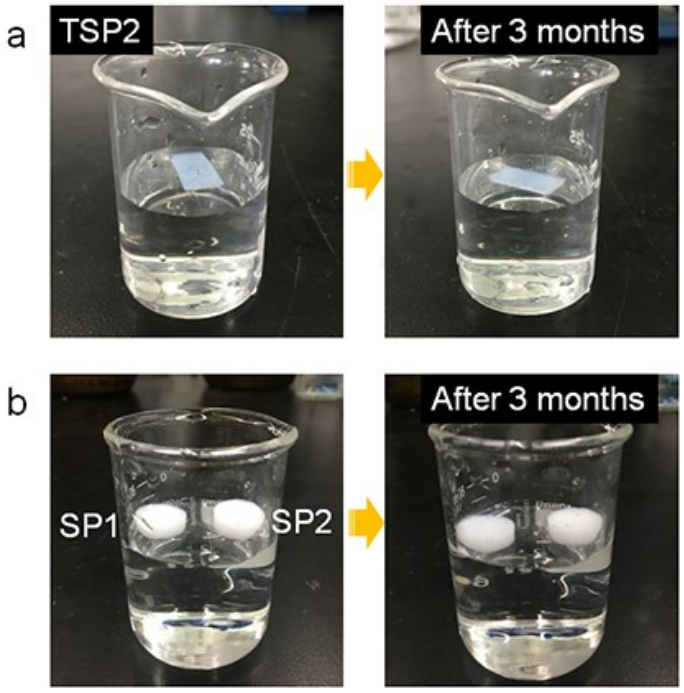

Figure S11. Contact of typical starch/polyorganosiloxane and TOS/polyorganosiloxane biocomposite aerogels with water. Because of their low bulk densities and high hydrophobicity, the obtained biocomposite aerogels float on top of water and remain floating on top of water after 3 months, showing excellent water resistance.

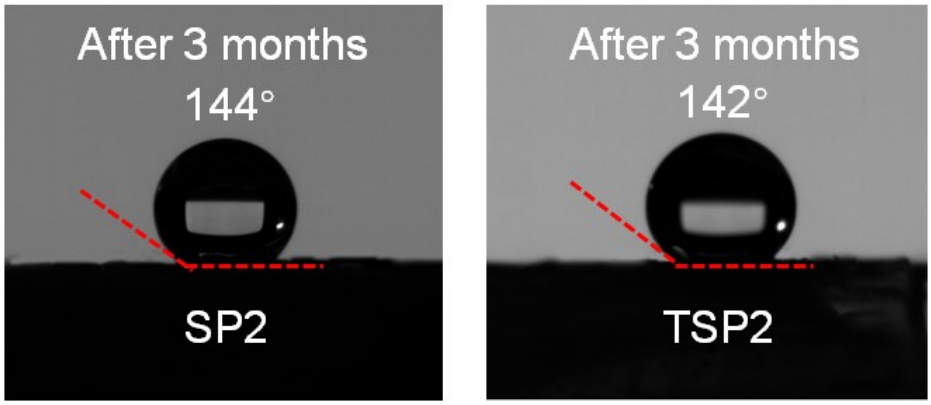

Figure S12. Water contact angles of typical starch/polyorganosiloxane and TOS/polyorganosiloxane biocomposite aerogels after being exposed to air for 3 months, which are almost the same as those of pristine aerogels, indicating the environmentally stable hydrophobicity of the biocomposite aerogels.

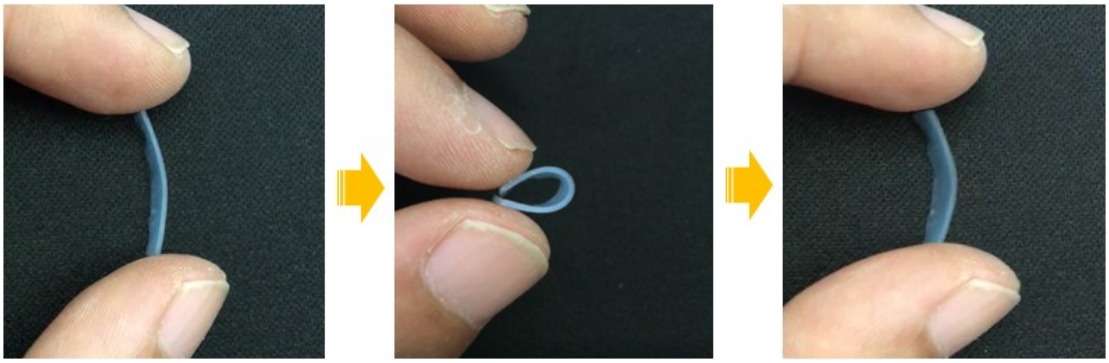

Figure S13. Photographs of a hand bending test on TSP2 after being exposed to air for 3 months. It maintains high bending flexibility after being exposed to air for 3 months, indicating the environmentally stable mechanical properties of the TOS/polyorganosiloxane biocomposite aerogels.

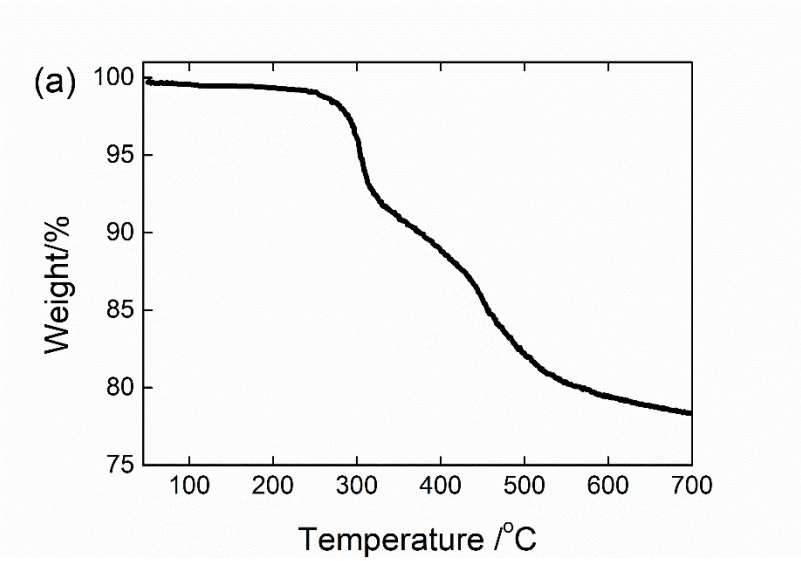

Figure S14. TG curves of TSP2 in air. Decomposition of TOS and methyl groups is supposed to occur above 250 °C, resulting in an apparent weight loss.

References

[1] A. C. Pierre, G. M. Pajonk, *Chem. Rev.* **2002**, *102*, 4243−4265.